American Mineralogist, Volume 81, pages 1396–1404, 1996

Periodic and nonperiodic interstratification in the chlorite-biotite series

HUIFANG XU,* YIQIANG ZHANG,† AND DAVID R. VEBLEN

Department of Earth and Planetary Sciences, Johns Hopkins University, Baltimore, Maryland 21218, U.S.A.

ABSTRACT

A systematic TEM investigation of interstratified chlorite-biotite crystals showed that the crystals are composed of domains of periodically interstratified chlorite-biotite, nonperiodically interstratified chlorite-biotite, biotite, and chlorite. The interstratified chlorite-biotite occurs as a vein filling and was apparently crystallized from a hydrothermal solution. The complex structure of the interstratified chlorite-biotite presumably results from a nonlinear growth phenomenon occurring under a nonequilibrium state.

A simple nonlinear dynamics model derived from Duffing's equation was constructed with an additional chemical potential that accounts for the variation of structural configuration of tetrahedral sheets or 2:1 layers in chlorite and biotite, a simple periodic fluctuation of hydrothermal fluid composition, and a simple damping force for two-dimensional lattice misfit on (001) resulting from the intergrowth of different types of layers with different structural configurations and other dissipation effects. Solutions to the equations of the model show that periodic interstratification, nonperiodic interstratification, and domains of the two end-member components (biotite, chlorite) can be formed during crystallization under various conditions. The nonperiodic sequences of biotite and chlorite layers along the c axis in the interstratified crystals produced by this model are chaotic rather than random. The calculations suggest that both periodic and nonperiodic interstratifications can result from periodic external force, e.g., compositional fluctuation of the fluid.

INTRODUCTION

Interstratification in phyllosilicates is a common phenomenon involving the intergrowth of two types of silicate layers (unit layers) or silicate and hydroxide layers, which are arranged along the c axis in either a periodic or a nonperiodic sequence. Regularly (periodically) interstratified phyllosilicate minerals are commonly intergrown with pure domains of one or both of their component layers. An interstratified mineral with a relatively ordered layer sequence along the c axis (CV < 0.75) may be considered a valid mineral species and given a mineral name (Bailey 1982). Several interstratified minerals occur in nature (see review paper by Bailey 1982): chlorite-talc (kulkeite, Schreyer et al. 1982), cookeite-pyrophyllite (lunijianlaite, Kong et al. 1990), smectite-illite (rectorite, Reynolds and Hower 1970, Veblen et al. 1990), chlorite-smectite (corrensite for the trioctahedral species, April 1981, Shau et al. 1990, Hiller 1993; and tosudite for the dioctahedral species, Brown et al. 1974), interstratified pyrophyllite-donbassite (Xu et al. 1994), interstratified chlorite-serpentine (Bailey et al. 1995; Xu and Veblen 1996), and interstratified chlorite-mica (Lee and Peacor 1985; Maresch et al. 1985).

Irregular (nonperiodic) mixed layering between chlorite and biotite is common in biotite-chlorite replacement reactions (e.g., Veblen and Ferry 1983; Olives Baños and Amouric 1984; Olives Baños et al. 1983; Eggleton and Banfield 1985; Maresch et al. 1985; Amouric et al. 1988). Interstratified chlorite-biotite formed during replacement reactions may exhibit strain between neighboring layers and contain inclusions precipitated between the layers (Veblen and Ferry 1983). Interstratification in the chlorite-wonesite series is also complex (Veblen 1983) and may be an intergrowth structure formed during crystallization, rather than a replacement reaction. The presence of irregular mixed layering in the chlorite-biotite system also causes nonstoichiometry of chlorite and biotite crystals. It is common to find chloritic minerals with abnormal compositions or optical properties in low-grade metamorphic or hydrothermally altered rocks as a result of fine-scale intergrowth, mixed layering, or both in the structure. Some chlorite samples contain significant amounts of Na, K, and Ca (e.g., Laird 1988) and exhibit abnormal optical properties (Albee 1962). Similar phenomena are common in biotite.

Few periodically interstratified chlorite-biotite mixed-layer materials have been reported. Eroshchev-Shak (1970) reported a fairly periodic 1:1 chlorite-biotite and concluded that it was formed by vermiculitization of biotite and subsequent chloritization of the vermiculite lay-

* Present address: Department of Geology, Arizona State University, Tempe, Arizona 85287-1404, U.S.A.

† Present address: S.S. Papadopulos & Associates, Inc., 7944 Wisconsin Avenue, Bethesda, Maryland 20814, U.S.A.

0003–004X/96/1112–1396$05.00

ers. Maresch et al. (1985) investigated an interstratified chlorite-biotite containing domains of periodic 1:1 structure with the use of high-resolution transmission electron microscopy (HRTEM), X-ray diffraction (XRD), and electron microprobe analysis. They concluded that the materials were alteration products formed during replacement of chlorite by biotite. All reported periodically interstratified chlorite-biotite structures occur in relatively low-temperature chlorite and biotite assemblages.

One-dimensional HRTEM-image simulations of a 1:1 interstratified chlorite-phlogopite structure show that HRTEM images can directly represent the crystal structure at the optimum defocus condition (Guthrie and Veblen 1990). We describe regularly (periodically) interstratified 1:1 chlorite-biotite and irregularly (nonperiodically) interstratified chlorite-biotite that have been characterized by selected-area electron diffraction (SAED), HRTEM, analytical electron microscopy (AEM), and simulated images, and present a model for the formation of these interstratifications.

Sample description and experimental methods

The weakly chloritized and biotitized actinolite used for this TEM study was collected from an altered norite-pegmatite dike at Blackhill Mountain near Chengde, Hebei, northern China. There are very fine platelets and veinlets of greenish biotite, chlorite, and brown biotite-like phyllosilicates within the uralitic actinolite. Other coexisting minerals are magnetite, apatite, and quartz. The vein-filling texture of the phyllosilicates is consistent with crystallization directly from hydrothermal fluid or by fluid-mediated reactions involving other minerals, rather than a solid-state topotactic replacement reaction.

Specimens for TEM investigation, which were selected from areas of a petrographic thin section containing fine-grained veins of the phyllosilicates, were thinned by argon ion milling. All TEM and AEM investigations were performed with a Philips 420ST electron microscope operated at 120 keV and equipped with an EDAX energy-dispersive X-ray detector and a Princeton Gamma-Tech system analyzer, as described by Veblen and Bish (1988) and Livi and Veblen (1987). All Fe was assumed to be Fe^{2+} in the interpretation of AEM analyses.

TEM observations of interstratified chlorite-biotite

An SAED pattern of the brown phyllosilicate (Fig. 1A) shows a period of 24.3 Å along the c^* direction, with >20 orders of 00l diffraction spots. Diffraction spots in 0kl ($k \neq 3n$) rows are strongly streaked, indicating highly disordered stacking involving layer shifts. The diffraction pattern can be indexed as a b^*-c^* reciprocal lattice plane for a phyllosilicate with stacking disorder. The corresponding HRTEM image (Fig. 1B) obtained at underfocus shows one-dimensional lattice fringes with a period of 24.3 Å (i.e., the d_{001} value). The HRTEM image also shows a few nonperiodic lattice fringes along the c axis,

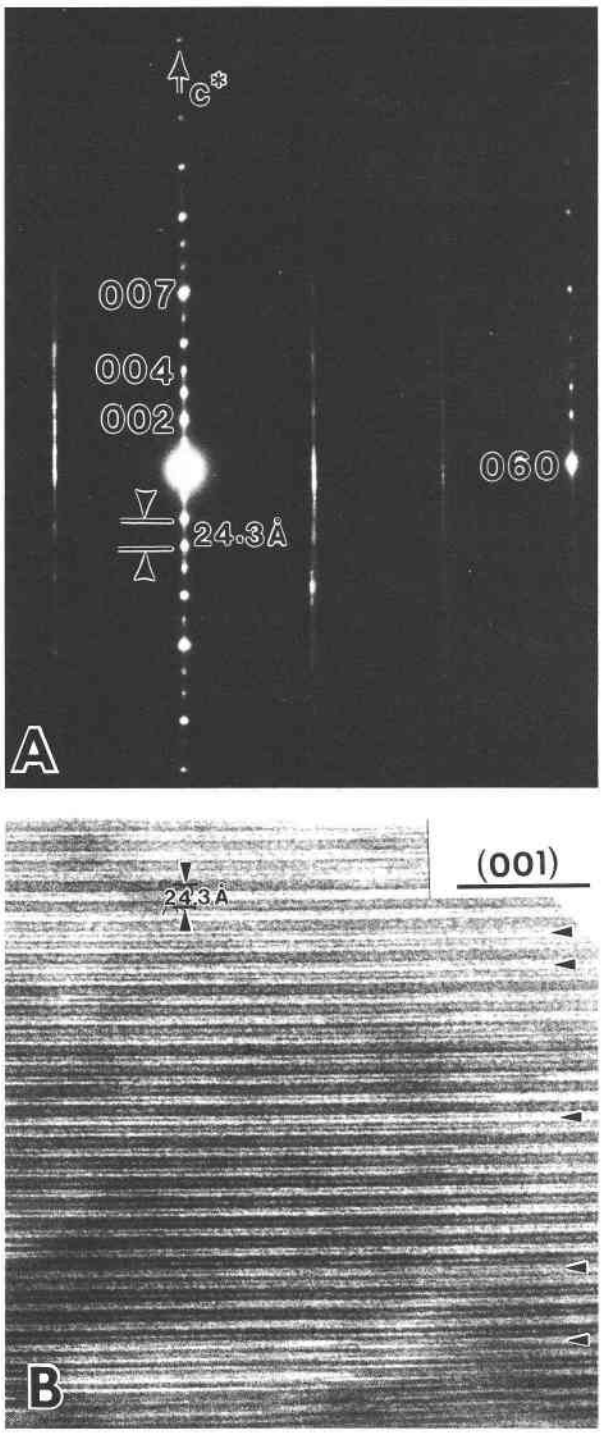

Figure 1. (**A**) SAED pattern showing the b^*-c^* reciprocal lattice plane of a periodically interstratified layer silicate. The 0kl ($k \neq 3n$) diffraction rows are strongly streaked. The measured values of d_{001} and d_{010} are 24.3 and 9.21 Å, respectively. (**B**) One-dimensional HRTEM image of the interstratified material at underfocus, showing the 24.3 Å periodicity of the (001) lattice fringes along the c^* direction. Some defects in the layer sequence (additional chlorite layers) are indicated by arrows.

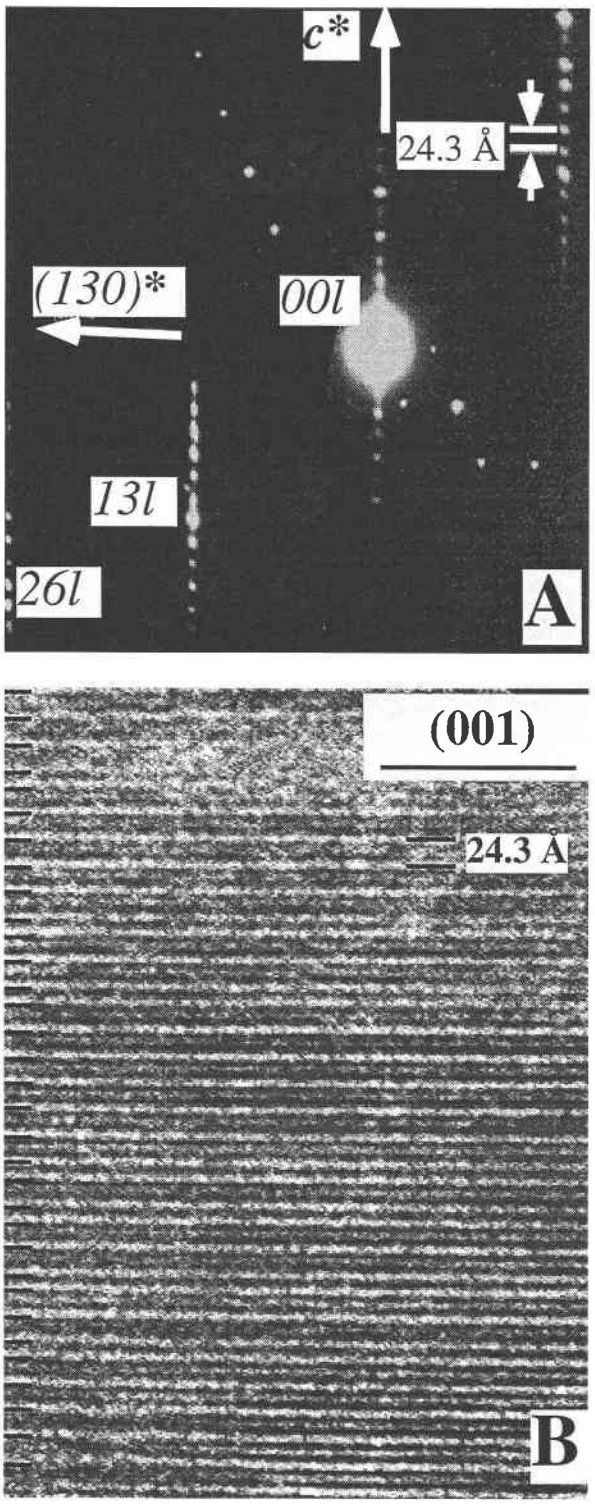

Figure 2. (**A**) SAED pattern of the interstratified phase with pseudo–a^*-c^* reciprocal lattice plane close to zone-axis orientation. There are relatively weak, diffuse streaks along the c^* direction. Other diffraction spots are from nearby actinolite. (**B**) One-dimensional HRTEM image corresponding to the SAED pattern in **A**, showing the 24.3 Å periodicity of the interstratified layer silicate.

which cause weak streaking of 00l and 06l diffraction spots parallel to the c^* direction.

An SAED pattern from another area corresponding to a pseudo–a^*-c^* reciprocal lattice plane also shows d_{001} = 24.3 Å but with much weaker streaking of the diffraction rows (Fig. 2A). A corresponding one-dimensional HRTEM image obtained at an overfocus condition shows a layer periodicity of 24.3 Å along the c^* direction (Fig. 2B). The HRTEM image also shows nonperiodic (001) lattice fringes that are related to weak streaking of the 00l, 13l, and 26l diffraction spots.

The 24.3 Å periodicity indicated by these SAED patterns and HRTEM images corresponds to the sum of the d_{001} values for chlorite (14.2 Å) and biotite (10.1 Å). The probable structure is regularly (periodically) interstratified 1:1 chlorite-biotite. Structural formulas of the interstratified material and coexisting chlorite and biotite calculated from AEM analyses are listed in Table 1. The composition corresponds quite well to that of a 1:1 molar mixture of chlorite and biotite and lies on the join between them (Fig. 3). This relationship is analogous to that of kulkeite, the composition of which lies between those of chlorite and talc (Schreyer et al. 1982). We conclude from the SAED patterns, HRTEM images, and AEM analyses that this material is an ordered, 1:1 chlorite-biotite mixed-layer silicate. A structural model of such periodically interstratified chlorite-biotite, constructed by alternating one chlorite layer and one biotite layer along the c axis, is shown in Figure 4. The AEM analyses suggest that the interlayer sites within biotite layers are almost completely filled by K and Na atoms, and all octahedral sheets are filled by Mg, Fe, and Al.

Experimentally at overfocus, it is easy to see the 24.3 Å layer periodicity of interstratified chlorite-biotite, which is consistent with the computer simulations of Guthrie and Veblen (1990) for interstratified 1:1 chlorite-phlogopite. In addition, the observed one-dimensional HRTEM images obtained at overfocus and underfocus fit the calculated one-dimensional HRTEM images of Guthrie and Veblen (Fig. 5). Thus, the simulations further support the interpretation of this material as a periodically interstratified 1:1 chlorite-biotite structure.

The strong streaking in 0kl ($k \neq 3n$) diffraction rows (Fig. 1A) is interpreted to result from $\pm\frac{1}{3}b$ stacking disorder within chlorite layers or $\pm 120°$ rotational stacking disorder within biotite layers analogous to those commonly observed in chlorite and biotite (Brown and Bailey 1962; Bailey 1988). Weak streaking of diffractions in 00l, 06l, 13l, and 26l rows parallel to the c^* direction is probably caused by extra chlorite layers, biotite layers, or both within the interstratified structure, as suggested by HRTEM images (Figs. 1B and 2B). Nonperiodic interstratification of chlorite and biotite layers contributes to the streaking of the 00l and 06l diffraction, and to the 02l and 04l diffraction along the c^* direction.

Nonperiodically interstratified mixed-layer chlorite-biotite is more abundant than periodically interstratified structure in the brown layer silicate of the sample.

TABLE 1. Structural formulas of the interstratified 1:1 chlorite-biotite and related minerals

Mineral	Structural formula
Actinolite	$(K_{0.05}Na_{0.26}Ca_{1.82})_{\Sigma 2.13}(Mg_{3.20}Fe_{1.55}Al_{0.24}Mn_{0.03})_{\Sigma 7.15}[(Si_{7.74}Ti_{0.01}Al_{0.25})_{\Sigma 8}O_{22}](OH)_2$
Biotite	$(K_{0.84}Na_{0.14}Ca_{0.04})_{\Sigma 1.02}(Mg_{1.44}Fe_{1.01}Al_{0.29}Mn_{0.00}Ti_{0.06})_{\Sigma 2.80}[(Si_{2.91}Al_{1.09})_{\Sigma 4}O_{10}](OH)_2$
Biotite	$(K_{0.82}Na_{0.12}Ca_{0.06})_{\Sigma 1.00}(Mg_{1.42}Fe_{1.02}Al_{0.26}Mn_{0.02}Ti_{0.07})_{\Sigma 2.79}[(Si_{2.92}Al_{1.08})_{\Sigma 4}O_{10}](OH)_2$
Biotite	$(K_{0.84}Na_{0.11}Ca_{0.04})_{\Sigma 0.99}(Mg_{1.43}Fe_{1.02}Al_{0.29}Mn_{0.01}Ti_{0.07})_{\Sigma 2.82}[(Si_{2.92}Al_{1.08})_{\Sigma 4}O_{10}](OH)_2$
Chl-Bi	$(K_{0.57}Na_{0.34}Ca_{0.27})_{\Sigma 0.91}(Mg_{4.43}Fe_{2.84}Al_{1.39}Mn_{0.05}Ti_{0.02})_{\Sigma 8.73}[(Si_{5.75}Al_{2.25})_{\Sigma 8}O_{20}](OH)_{10}$
Chl-Bi	$(K_{0.57}Na_{0.24}Ca_{0.16})_{\Sigma 0.97}(Mg_{4.48}Fe_{3.09}Al_{1.32}Mn_{0.00}Ti_{0.00})_{\Sigma 8.89}[(Si_{5.77}Al_{2.23})_{\Sigma 8}O_{20}](OH)_{10}$
Chl-Bi	$(K_{0.60}Na_{0.41}Ca_{0.19})_{\Sigma 1.01}(Mg_{4.64}Fe_{2.89}Al_{1.23}Mn_{0.02}Ti_{0.02})_{\Sigma 8.80}[(Si_{5.74}Al_{2.26})_{\Sigma 8}O_{20}](OH)_{10}$
Chlorite	$(Mg_{2.38}Fe_{2.44}Al_{1.12}Ca_{0.02})_{\Sigma 5.96}[(Si_{2.95}Al_{1.05})_{\Sigma 4}O_{10}](OH)_8$
Chlorite	$(Mg_{2.65}Fe_{2.36}Al_{1.12}Ca_{0.04})_{\Sigma 5.96}[(Si_{2.91}Al_{1.09})_{\Sigma 4}O_{10}](OH)_8$
Chlorite	$(Mg_{2.33}Fe_{2.40}Al_{1.14}Ca_{0.01})_{\Sigma 5.96}[(Si_{3.00}Al_{1.00})_{\Sigma 4}O_{10}](OH)_8$

Note: Formulas were determined from AEM analyses described in the text.

HRTEM images show areas dominated by biotite layers with nonperiodic interstratification of chlorite and biotite layers (Fig. 6A). In contrast, other HRTEM images show the crystal with both chlorite-dominant and nonperiodic interstratified domains (Fig. 6B). Some areas display nonperiodic intergrowth of chlorite and biotite domains (Fig. 6C). An SAED pattern from the nonperiodic chlorite-dominant area shows streaking of the 00*l* rows (Fig. 7C).

None of the interstratified chlorite-biotite crystals we examined was completely periodic, and the type of disorder varied between crystal grains and even in different areas within a crystal. In general, the interstratified chlorite-biotite material can be considered a "mixed crystal" composed of chlorite domains, biotite domains, periodically interstratified domains, and nonperiodically interstratified domains, all intergrown along the *c* axis. SAED patterns from nonperiodic biotite-dominant areas are characterized by strong diffraction spots at biotite diffraction positions and streaks along the *c** direction (Fig. 7A); patterns from areas dominated by periodically interstratified chlorite-biotite show streaked diffraction spots characteristic of 24 Å periodicity (Fig. 7B); and those from nonperiodic chlorite-dominant areas show strong diffraction spots at chlorite diffraction positions and streaking along the *c** direction (Fig. 7C). The most complex SAED patterns are from areas composed of all these possible variations: chlorite, biotite, periodically interstratified, and nonperiodically interstratified domains (Fig. 7D). The feature in the SAED pattern of Figure 7D is different from features in periodic and random oscillations in spectrum space according to the results of Baker and Gollub (1990). Such a phenomenon is a reliable indicator of chaos, even though it does not guarantee sensitivity to initial conditions (Baker and Gollub 1990).

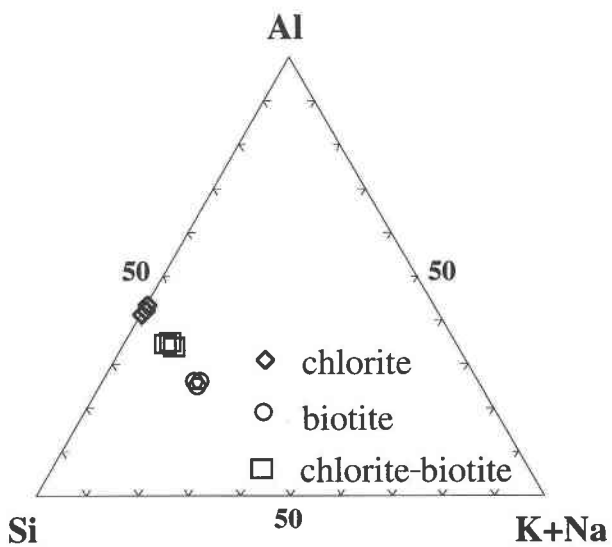

FIGURE 3. Ternary plot of the interstratified layer silicate (labeled chlorite-biotite) and its related chlorite and biotite in the (K,Na)-Al-Si ternary system.

GENESIS OF THE OBSERVED INTERSTRATIFIED STRUCTURES

Mechanisms for the formation of interstratified structures

Interstratified structures containing chlorite and biotite layers can form in several ways. In many cases, they appear to result from partial replacement of one mineral by another, for example, from reactions of biotite to chlorite (Veblen and Ferry 1983; Olives Baños and Amouric 1984; Olives Baños et al. 1983; Eggleton and Banfield

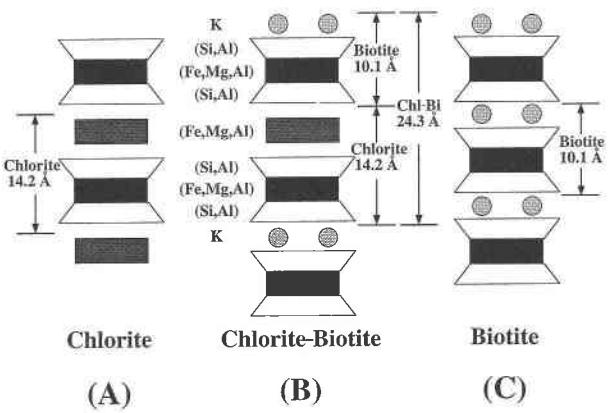

FIGURE 4. Structural model of the interstratified 1:1 chlorite-biotite (**B**), based on regular interlayering of chlorite and biotite layers. The structures of chlorite and biotite are also illustrated for comparison (**A** and **C**, respectively).

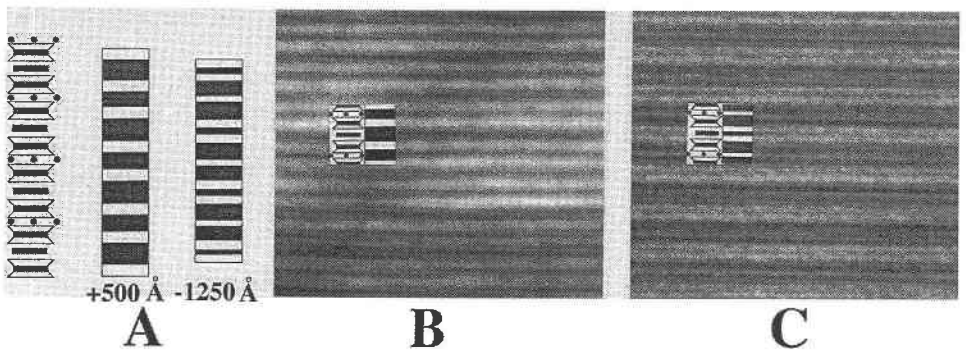

FIGURE 5. Comparison of simulated one-dimensional HRTEM images of 1:1 chlorite-phlogopite at underfocus (−1250 Å) and overfocus (+500 Å) conditions (from Guthrie and Veblen 1990) (**A**) with experimental one-dimensional HRTEM images obtained under these conditions (**B** and **C**). The insets in **B** and **C** show both the structural models and calculated images from **A**.

1985) or from reactions of chlorite to biotite (Maresch et al. 1985). Similarly, previous studies have reported that interstratified 1:1 chlorite-biotite forms as an alteration product during chloritization of biotite (Olives Baños 1985), biotitization of chlorite (Maresch et al. 1985), or vermiculitization of biotite with subsequent chloritization of vermiculite layers (Eroshchev-Shak 1970).

More generally, the occurrence of periodically interstratified phyllosilicates (including 1:1 chlorite-biotite) has been explained in several ways. For example, the mixed-layer silicate can (1) grow as a thermodynamically stable phase; (2) form as an intermediate structure during a solid-state reaction from one layer silicate to another (Hower et al. 1976; Maresch et al. 1985); (3) form by direct growth as a result of a periodic oscillation in hydrothermal solution composition (Kong et al. 1990); or (4) appear as an artifact of interparticle diffraction from an assembly of fundamental particles (Nadeau et al. 1984). There are also variations of the above explanations, such as the Axial Next-Nearest-Neighbor Ising (ANNNI) model for periodically interstratified phyllosilicates (Zen 1967), which is an example of growth of a thermodynamically stable or metastable phase. On the basis of the ANNNI model, high-temperature conditions favor formation of interstratified phyllosilicates (Zen 1967). However, interstratified phyllosilicates commonly occur in low-temperature conditions.

Recent TEM studies of interstratified smectite-illite (Veblen et al. 1990; Ahn and Peacor 1986, 1989), chlorite-talc (Schreyer et al. 1982), cookeite-pyrophyllite (Kong et al. 1990, 1992), pyrophyllite-donbassite (Xu et al. 1994), and the directly crystallized chlorite-biotite reported here have shown that periodically interstratified phyllosilicates can be composed of mixtures of periodically interstratified domains with a thickness considerably greater than those of fundamental particles, nonperiodically interstratified domains, and domains of one or both end-member structures. Like other interstratified phyllosilicates, the 1:1 chlorite-biotite does not grow as large homogeneous crystals but rather as one part of a mixed crystal containing biotite, chlorite, and nonperiodically interstratified chlorite-biotite. We propose that the interstratified chlorite-biotite is a growth structure resulting from the rapid coprecipitation of chlorite and biotite from hydrothermal solution. There is no thermodynamic stability field for the interstratified structure with respect to chlorite and biotite. This allows us to propose a nonlinear dynamics model for the crystallization of the chlorite-biotite intergrowths observed in this study. In this nonequilibrium crystallization model, chlorite, biotite, and the periodic and nonperiodic mixed-layer structures can result from periodic fluctuations in fluid composition. The original equation describing this kind of structural oscillation was introduced to describe the hardening spring effect observed in many mechanical oscillations (Duffing 1918). Since then, the equation has become one of the most common examples in text books and research articles about nonlinear oscillation (Guckenheimer and Holmes 1983; Baker and Gollub 1990). Similar dynamical oscillation models were also applied to magneto-elastic oscillation (Guckenheimer and Holmes 1983) and to chemical oscillation in minerals (Jamtveit 1991). Dynamical oscillation models have also been applied to intergrowths of periodic and nonperiodic polytypic structures at the unit-cell scale (Vignoles 1992; Xu and Veblen 1995).

Formulation of the nonlinear crystallization model

We followed Jamtveit (1991) and Xu et al. (1995) in the development of our formulation for this system. In general, we use two separate potentials (G) relating to the structural configuration (or distortion) for chlorite and biotite. With these simple chemical potentials it is assumed that the additional energy of biotite and chlorite layers is related to the difference in the structural configurations (u) of biotite and chlorite, e.g., the configuration of tetrahedral sheets. The configuration parameter (u) of the boundary between bonded chlorite and biotite layers on the (001) plane is set to zero. The proposed potentials are expressed as follows:

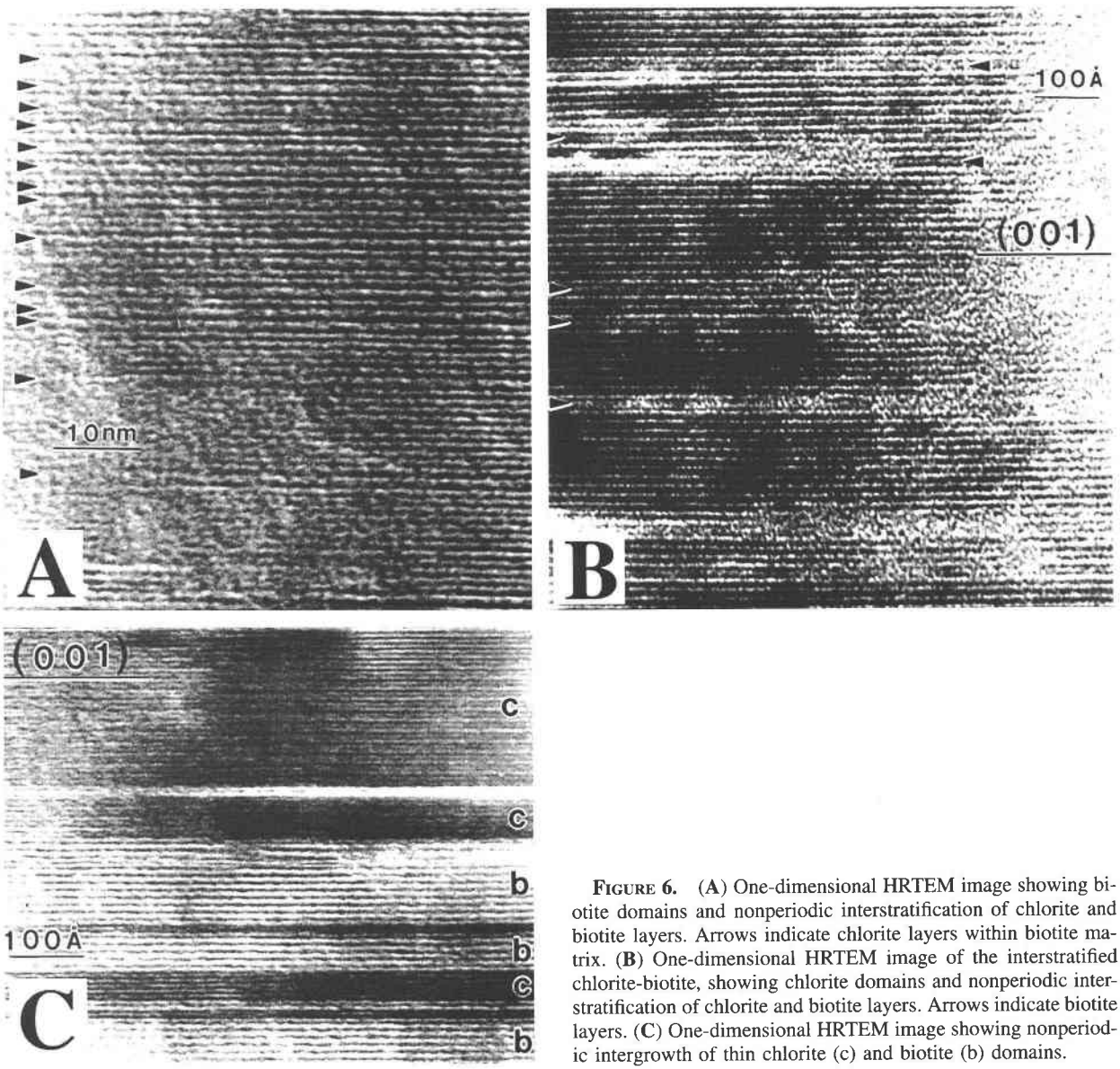

FIGURE 6. (**A**) One-dimensional HRTEM image showing biotite domains and nonperiodic interstratification of chlorite and biotite layers. Arrows indicate chlorite layers within biotite matrix. (**B**) One-dimensional HRTEM image of the interstratified chlorite-biotite, showing chlorite domains and nonperiodic interstratification of chlorite and biotite layers. Arrows indicate biotite layers. (**C**) One-dimensional HRTEM image showing nonperiodic intergrowth of thin chlorite (c) and biotite (b) domains.

$$G(u) = G_0 + \beta[a_1(u/2 + 0.5 - b)^2 - \ln(u/2 + 0.5 + \delta)]$$

for biotite (1a)

$$G(u) = G_0 + \beta[a_1(0.5 - u/2 - b)^2 - \ln(0.5 - u/2 + \delta)]$$

for chlorite (1b)

where u is the scaled structure parameter characterizing the structural difference (e.g., tetrahedral sheets) of chlorite and biotite; G_0 is the normalized energy of chlorite and biotite without any structural distortion; and β, a_1, b, and δ are adjustable parameters for the assumed potential functions. A logarithmic function for the potentials was used to avoid an extreme distortion of the crystal structures in biotite and chlorite. The basic forms of the two potentials are illustrated in Figure 8. The two potential wells represent the stable chlorite and biotite configurations. The model assumes that the interstratification occurs only in a system with both chlorite and biotite crystallizing from solution as thermodynamically stable structures. The model simulation is based on the simple potential functions with the potential minima within the u values between -1 and 1, which is a function of temperature and other conditions. We assume that the two-dimensional structural configuration of chlorite and biotite is continuous and, therefore, that the chemical potential for the chlorite-biotite system is also continuous. The potential at $-0.1 \leq u \leq +0.1$ is considered to be parabolic in form, i.e., $A - B(u/2)^2$ (Fig. 8), so that the potential is continuous for all u values. The pseudocontinuous potential may then be rewritten as follows:

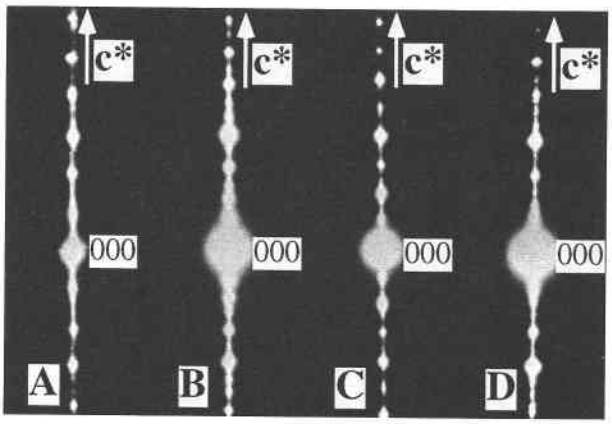

FIGURE 7. Series of 00*l* electron diffraction rows from parts of an interstratified "crystal" dominated by biotite layers (**A**), periodically interstratified domains (**B**), chlorite layers (**C**), and more complex intergrowth of different domain types (**D**). Streaking of diffraction spots along c^* was caused by nonperiodic interstratification of chlorite and biotite layers.

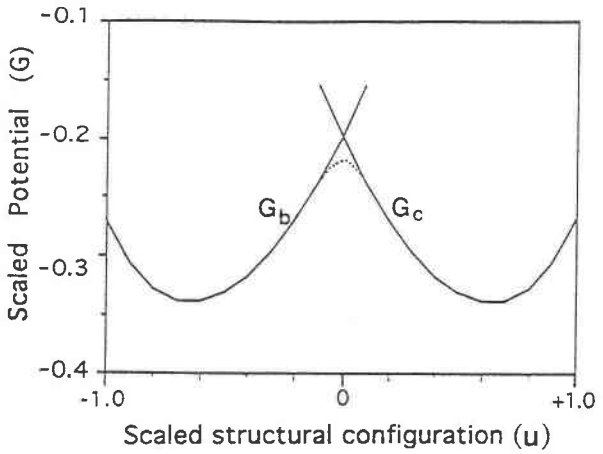

FIGURE 8. Proposed chemical potentials as functions of the scaled structural configuration (u) between biotite and chlorite in the chlorite-biotite system.

$$G(u) = G_0 + \beta[a_1(u/2 + 0.5 - b)^2 - \ln(u/2 + 0.5 + \delta)]$$
$$\text{for } -1.0 \le u \le -0.1 \quad (2a)$$

$$G(u) = G_0 + \beta[A - B(u/2)^2]$$
$$\text{for } -0.1 \le u \le +0.1 \quad (2b)$$

$$G(u) = G_0 + \beta[a_1(0.5 - u/2 - b)^2 - \ln(0.5 - u/2 + \delta)]$$
$$\text{for } +0.1 \le u \le 1.0 \quad (2c)$$

where A and B are parameters from the two basic potentials of Equation 1, so that the potential is continuous. Thus, a layer with the structural configuration $u < 0$ corresponds to biotite, and a layer with $u > 0$ corresponds to chlorite. According to Guckenheimer and Holmes (1983) and Jamtveit (1991), the driving force for crystallization resulting from the proposed potential is given by

$$-\nabla G(u) = \ddot{u} \quad (3)$$

or

$$\nabla G(u) + \ddot{u} = 0 \quad (4)$$

$$\nabla G(u) = \beta[2a_1(u/2 + 0.5 - b) - 1/(u/2 + 0.5 + \delta)]$$
$$\text{for } -0.1 \le u \le -0.1 \quad (5a)$$

$$\nabla G(u) = -\beta B u$$
$$\text{for } -0.1 \le u \le +0.1 \quad (5b)$$

$$\nabla G(u) = \beta[2a_1(0.5 - u/2 - b) - 1/(0.5 - u/2 + \delta)]$$
$$\text{for } +0.1 \le u \le 1.0. \quad (5c)$$

The driving force tends to minimize the energy of the crystals during crystallization, i.e., by forming structural configurations of chlorite and biotite layers with minimum potentials. Additional energy is introduced between neighboring layers as a result of the structural differences between chlorite and biotite. The additional force is assumed to be proportional to the structural variation ($\sigma\dot{u}$) between neighboring tetrahedral sheets in the crystal. This assumption is similar to that proposed by Jamtveit (1991) for a compositional oscillation system. Addition of the term $\sigma\dot{u}$ (a damping term) to the above equation results in the following equation:

$$\nabla G(u) + \ddot{u} + \sigma\dot{u} = 0. \quad (6)$$

Equation 6 describes a damped structural oscillation without an external force (i.e., an equilibrium state). If the system is not at equilibrium, there is also an external force (e.g., compositional fluctuation of the fluid) influencing crystallization. We assume that the external force is a simple periodic fluctuation, $F = \gamma \cos(\omega t)$, consistent with one of the proposed mechanisms for periodic interstratification of cookeite and pyrophyllite (i.e., a periodic change in fluid composition: Kong et al. 1990). The parameter γ is adjustable and characterizes the amplitude of the fluctuation of the fluid composition. The value of γ is zero only at equilibrium. The parameters ω and t are the oscillation frequency of fluid composition and the time from the start of crystallization, respectively. Addition of the periodic external force, $F = \gamma \cos(\omega t)$, to the above equation, results in Equation 7:

$$\nabla G(u) + \ddot{u} + \sigma\dot{u} = \gamma \cos(\omega t). \quad (7)$$

Equation 7, Duffing's equation, describes a forced oscillation (Guckenheimer and Holmes 1983; Thompson and Stewart 1986; Xu et al. 1995), which may be rewritten as the following autonomous system of equations (Guckenheimer and Holmes 1983; Jamtveit 1991):

$$\dot{u} = v \quad (8a)$$

$$\dot{v} = -\nabla G(u) - \sigma v + \gamma \cos(\omega\theta) \quad (8b)$$

$$\dot{\theta} = 1. \quad (8c)$$

All variables in Equation 8 are dimensionless. The vari-

able v is the rate of change of the structural configuration (u), and θ is the elapsed time. The equations, which can be solved numerically, represent a nonlinear structural oscillation with damping and an external force (i.e., a nonequilibrium state).

Results of the nonlinear crystallization model

General solutions to these equations exhibit nonperiodic oscillations and are very sensitive to initial conditions (i.e., the structural configuration of the matrix) (Thompson and Stewart 1986; Baker and Gollub 1990). The structure of these nonperiodic oscillations (or the intergrowth of chlorite and biotite layers) is not random (or totally disordered); it is chaotic, which is a type of nonperiodic structure with a degree of order (Hao 1984; Baker and Gollub 1990). Some typical numerical solutions are illustrated in Figure 9; the negative and positive u values of the structural configurations in these figures correspond to oscillations (or intergrowths) between biotite and chlorite layers in the mixed crystal. Thus, nonperiodic structural oscillations in the mixed crystal result from periodic chemical oscillations corresponding to fine-scale, nonperiodic interstratification of chlorite and biotite layers (Fig. 9A) or intergrowths of small chlorite and biotite domains (Fig. 9B). When the system is close to equilibrium (i.e., $\gamma \approx 0$) or at equilibrium ($\gamma = 0$), there are stable solutions, which correspond to separate coexisting crystals of chlorite and biotite with structures of minimum potentials. Only under certain conditions is there a periodic oscillation of chlorite and biotite layers (Fig. 9C), corresponding to the ordered, 1:1 mixed-layer chlorite-biotite structure observed in this study. The numerical results are similar to the observed TEM results of Figures 1 and 6.

During the growth of a real crystal, the situation may be more complex. The external conditions (e.g., fluid composition, temperature, etc.) may change during crystallization, and the resulting crystal may exhibit an intergrowth of several structures that reflect these changes. A crystal formed by nonequilibrium crystallization could consist of periodically interstratified domains, nonperiodically interstratified domains, and both chlorite and biotite domains, similar to those observed.

On the basis of the above nonlinear oscillation model, interstratified phyllosilicates that form by direct crystallization occur only under a sufficiently strong external force. Requirements for interstratification include (1) two end-member structures that are similar, at least in the plane of intergrowth (i.e., a small damping force), and (2) nonequilibrium conditions (i.e., a sufficiently large external force). Crystallization at low temperatures may more commonly result in larger deviations from equilibrium than high-temperature crystallization. Thus, low-temperature crystallization favors the formation of the interstratified structures. This fact is consistent with the observation that interstratified layer silicates form under low-temperature conditions, whereas high-temperature processes typically produce relatively well-ordered layer silicates consisting of a single layer type, such as mica and chlorite crystals. The proposed oscillation model may also be applied to interstratified illite-smectite that precipitated in the presence of solution.

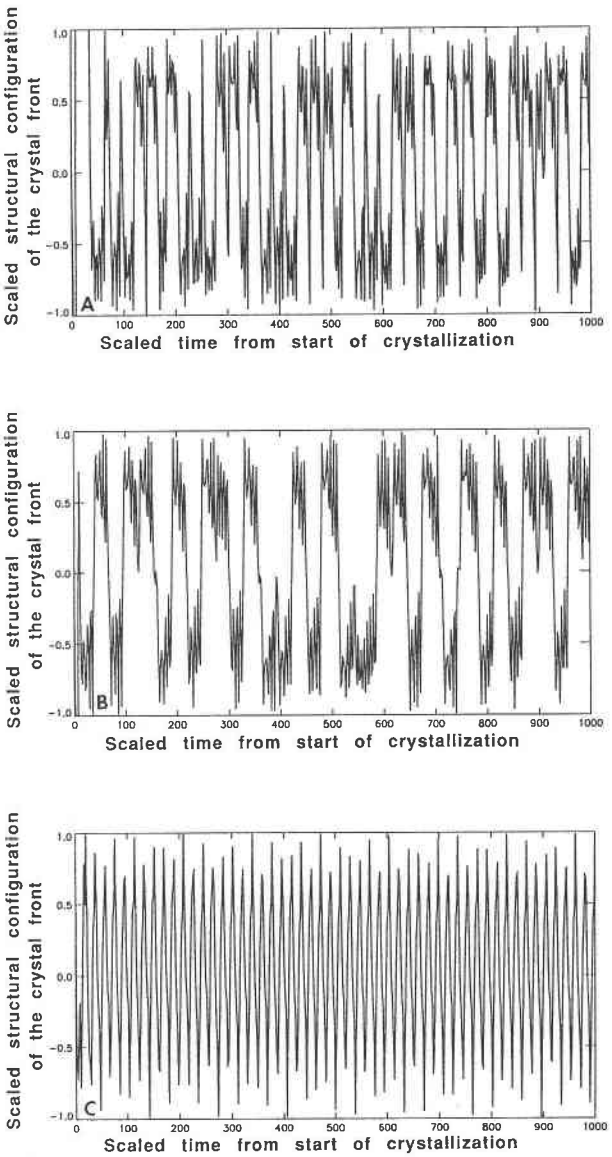

FIGURE 9. Numerical solutions of the equations at nonequilibrium states, showing nonperiodic oscillation (interstratification) of chlorite and biotite layers (**A**), intergrowth of chlorite and biotite domains (**B**), and periodic oscillation (interstratification) of chlorite and biotite layers (**C**). Parameters for the above solutions are (**A**) $\gamma = 0.11$, $\sigma = 0.09$, $\omega = 1$, $\beta = 0.03$; (**B**) $\gamma = 0.08$, $\sigma = 0.12$, $\omega = 1$, $\beta = 0.03$; (**C**) $\gamma = 0.03$, $\sigma = 0.4$, $\omega = 1$, $\beta = 0.03$. The structural configurations with positive and negative u values correspond to chlorite and biotite layers, respectively.

ACKNOWLEDGMENTS

We appreciate useful discussions with John Ferry and Ken Livi. The paper benefited immensely from thorough reviews by Bill Carey, George

Guthrie, and an anonymous reviewer. This work was supported by NSF grant EAR-8903630 and DOE grant DE-FG02-89ER14074. Gufeng Luo of Nanjing University is thanked for his help during the field work of H.X. Electron microscopy was performed in the HRTEM/AEM laboratory at Johns Hopkins University, which was established with partial support from NSF grant EAR-8300365.

References cited

Ahn, J.H., and Peacor, D.R. (1986) Transmission and analytical electron microscopy of the smectite-to-illite transition. Clays and Clay Minerals, 34, 165–179.

———(1989) Mixed-layer illite/smectite from Gulf Coast shales: A reappraisal of TEM images. Clays and Clay Minerals, 37, 542–546.

Albee, A.L. (1962) Relationships between the mineral association, chemical composition and physical properties of the chlorite series. American Mineralogist, 47, 851–870.

Amouric, M., Gianetto, I., and Proust, D. (1988) 7, 10, and 14 Å mixed-layer phyllosilicates studied structurally by TEM in pelitic rocks of the Piemontese zone (Venezuela). Bulletin de Minéralogie, 104, 298–313.

April, R.H. (1981) Trioctahedral smectite and interstratified chlorite/smectite in Jurassic strata of the Connecticut Valley. Clays and Clay Minerals, 29, 31–39.

Bailey, S.W. (1982) Nomenclature for regular interstratifications. American Mineralogist, 67, 394–398.

———(1988) X-ray diffraction identification of the polytypes of mica, serpentine, and chlorite. Clays and Clay Minerals, 36, 193–213. Cited in Stoker, J.J. (1950) Nonlinear vibrations in mechanical and electrical systems, 273 p. Interscience, New York.

Bailey, S.W., Banfield, J.F., Barker, W.W., and Katchan, G. (1995) Dozyite, a 1:1 regular interstratification of serpentine and chlorite. American Mineralogist, 80, 65–77.

Baker, G.L., and Gollub, J.P. (1990) Chaotic dynamics, 182 p. Cambridge University Press, New York.

Brown, B.E., and Bailey, S.W. (1962) Chlorite polytypism: I. Regular and semirandom one-layer structures. American Mineralogist, 47, 819–850.

Brown, G., Bourguigon, P., and Thorez, J. (1974) A lithium-bearing aluminian redular mixed layer montmorillonite-chlorite from Huy, Belgium. Clay Minerals, 10, 135–144.

Duffing, G. (1918) Erzwungene Schwingungen bei Vernderlicher Eigenfrequenz. Vieweg: Braunschweig.

Eggleton, R.A., and Banfield, J.F. (1985) The alteration of granitic biotite to chlorite. American Mineralogist, 70, 902–910.

Eroshchev-Shak, V.A. (1970) Mixed-layer biotite-chlorite formed in course of local epigenesis in the weathering crust of a biotite gneiss. Sedimentology, 15, 115–121.

Guckenheimer, J., and Holmes, P. (1983) Nonlinear oscillations, dynamical systems, and bifurcations of vector fields, 453 p. Springer-Verlag, New York.

Guthrie, G.D., Jr., and Veblen, D.R. (1990) Interpreting one-dimensional high-resolution transmission electron micrographs of sheet silicates by computer simulation. American Mineralogist, 75, 276–288.

Hao, B.-L. (1984) Chaos, 576 p. World Scientific, Singapore.

Hiller, S. (1993) Origin, diagenesis, and mineralogy of chlorite minerals in Devonian Lacustrine mudrocks, Orcadian basin, Scotland. Clays and Clay Minerals, 41, 240–259.

Hower, J., Eslinger, E.V., Hower, M.E., and Perry, E.A. (1976) Mechanism of burial metamorphism of argillaceous sediments: I. Mineralogical and chemical evidence. Geological Society of America Bulletin, 87, 725–737.

Jamtveit, B. (1991) Oscillatory zonation patterns in hydrothermal grossular-andradite garnet: Nonlinear dynamics in regions of immiscibility. American Mineralogist, 76, 1319–1327.

Kong, Y., Peng, X., and Tian, D. (1990) Lunijianlaite: A new regular interstratified mineral. Acta Mineralogica Sinica, 10, 289–298.

Kong, Y., Peng, X., Tian, T., and Wang, Y. (1992) HRTEM observation of fine structure of lunijianlaite. Acta Mineralogica Sinica, 12, 7–13.

Laird, J. (1988) Chlorite: Metamorphic petrology. In Mineralogical Society of American Reviews in Mineralogy, 19, 405–454.

Lee, J.H., and Peacor, D.R. (1985) Ordered 1:1 interstratification of illite and chlorite: A transmission and analytical electron microscopy study. Clays and Clay Minerals, 33, 463–467.

Livi, K.J.T., and Veblen, D.R. (1987) "Eastonite" from Easton, Pennsylvania: A mixture of phlogopite and a new form of serpentine. American Mineralogist, 72, 113–125.

Maresch, W.V., Massonne, H.-J., and Czank, M. (1985) Ordered and disordered chlorite/biotite interstratifications as alteration products of chlorite. Neues Jahrbuch für Mineralogie Abhandlungen, 152, 79–100.

Nadeau, P.H., Wilson, M.J., McHardy, W.J., Tait, J.M. (1984) Interparticle diffraction: A new concept for interstratified clays. Clay Minerals, 19, 757–769.

Olives Baños, J. (1985) Biotites and chlorites as interlayered biotite-chlorite crystals. Bulletin de Minéralogie, 108, 635–641.

Olives Baños, J., Amouric, M., De Fouquet, C., and Baronnet, A. (1983) Interlayering and interlayer slip in biotite as seen by HRTEM. American Mineralogist, 68, 754–758.

Olives Baños, J., and Amouric, M. (1984) Biotite chloritization by interlayer brucitization as seen by HRTEM. American Mineralogist, 69, 869–871.

Reynolds, R.C., Jr., and Hower, J. (1970) The nature of interlayering in mixed-layer illite-montmorillonite. Clays and Clay Minerals, 18, 25–36.

Schreyer, W., Medenbach, O., Abraham, K., Gebert, W., and Müller, W.F. (1982) Kulkeite, a new metamorphic phyllosilicate mineral: Ordered 1:1 chlorite/talc mixed-layer. Contributions to Mineralogy and Petrology, 80, 103–109.

Shau, Y.H., Peacor, D.R., and Essene, E.J. (1990) Corensite and mixed-layer chlorite/corensite in metabasalt from Northern Taiwan: TEM/AEM, EPMA, XRD, and optical studies. Contributions to Mineralogy and Petrology, 105, 123–142.

Thompson, J.M.T., and Stewart, H.B. (1986) Nonlinear dynamics and chaos: Geometrical methods for engineers and scientists, 376 p. Wiley, Chichester, U.K.

Veblen, D.R. (1983) Microstructures and mixed layering in intergrown wonesite, chlorite, talc, biotite, and kaolinite. American Mineralogist, 68, 566–580.

Veblen, D.R., and Ferry, J.M. (1983) A TEM study of the biotite-chlorite reaction and comparison with petrologic observations. American Mineralogist, 68, 1160–1168.

Veblen, D.R., and Bish, D.L. (1988) TEM and X-ray study of orthopyroxene megacrysts: Microstructures and crystal chemistry. American Mineralogist, 73, 677–691.

Veblen, D.R., Guthrie, G.D., Jr., Livi, K.J.T., and Reynolds, R.C., Jr. (1990) Highresolution transmission electron microscopy and electron diffraction of mixed-layer illite/smectite: Experimental results. Clays and Clay Minerals, 38, 1–13.

Vignoles, G.L. (1992) Atomic relaxation and dynamical generation of ordered and disordered CVI SiC polytypes. Journal of Crystal Growth, 118, 430–438.

Xu, H., Buseck, P.R., and Luo, G. (1994) Periodic and nonperiodic interstratification in the chlorite-pyrophillite series. Geological Society of America Abstracts with Programs, 26, A165.

Xu, H., and Veblen, D.R. (1995) Periodic and nonperiodic stacking in biotite from the Bingham Canyon porphyry copper deposit, Utah. Clays and Clay Minerals, 43, 159–173.

Xu, H., Veblen, D.R., and Zhang, Y. (1995) Structural modulation and phase transition in a Na-rich alkali feldspar. American Mineralogist, 80, 897–906.

Xu, H., and Veblen, D.R. (1996) Interstratification and other reaction microstructures in the chlorite-berthierine series. Contributions to Mineralogy and Petrology, in press.

Zen, E-an (1967) Mixed-layer minerals as one-dimensional crystals. American Mineralogist, 52, 635–660.

Manuscript received July 7, 1994
Manuscript accepted July 16, 1996